Submitted to the 2010 Proc. of the SPIE, To Appear.

Quantifying the Benefit of Airborne and Ground Sensor Fusion for Target Detection

Alina Zare[a], Miranda Silvious[b], Ryan Close[a], and Paul Gader[a]

[a]Department of Computer and Information Science and Engineering, University of Florida, Gainesville, FL, USA;
[b]U.S. Army RDECOM CERDEC, Ft. Belvoir, VA, USA

ABSTRACT

In this paper, a study involving the detection of buried objects by fusing airborne Multi-Spectral Imagery (MSI) and ground-based Ground Penetrating Radar (GPR) data is investigated. The benefit of using the airborne sensor to cue the GPR, which will then search the area indicated by the MSI, is investigated and compared to results obtained via a purely ground-based system. State-of-the-art existing algorithms, such as hidden Markov models will be applied to the GPR data both in queued and non-queued modes. In addition, the ability to measure disturbed earth with the GPR sensor will be investigated. Furthermore, state-of-the-art algorithms for the MSI system will be described. These algorithms require very high detection rates with acceptable false alarm rates in order to serve as an acceptable system. Results will be presented on data collected at outdoor testing and evaluation sites.

Keywords: Ground Penetrating Radar, Airborne Imaging, Sensor Fusion

1. INTRODUCTION

In this paper, the potential of using airborne Multi-Spectral Imagery (MSI) to cue a ground-based ground penetrating radar (GPR) system for buried landmine detection is investigated. Using the airborne Multi-Spectral imagery, algorithms were developed in order to generate alarms from the airborne imagery. These airborne alarms were used to cue ground-based GPR alarms if they fall within a one meter halo of an airborne alarm. GPR alarms were created using four algorithms and the results are shown both with and without cueing from the airborne imagery. Additionally, a method to generate disturbed earth maps using GPR data is described. The overall goal of cueing the GPR system is to increase the rate of advance of the ground-based GPR system by focusing analysis only on regions cued by the airborne MSI data. Results are scored and provided for data from an area covering approximately 0.5 linear kilometers.

2. MULTI-SPECTRAL IMAGE ANALYSIS

The MSI data contains three bands corresponding to three wavelengths that aid in the detection of disturbed earth. Specifically, the pixel-wise ratio of the first two bands highlights disturbed earth in the imaged scene. An example of a disturbed earth ratio image computed using MSI is shown in Figure 2.

As can be seen in Figure 2, disturbed soil effects from vehicle tracks in the road (evidenced by the linear features in figure 2) are highlighted in the ratio image as well as disturbed soil from targets and refilled holes. In order to highlight areas associated with targets and refilled holes, anamoly detection using a double-gated filter followed by background subtraction was utilized. The double-gated filter performed anomaly detection by convolving the image with target and background structuring elements. The difference of the convolutions from the target and background structuring elements resulted in the double-gated filter results. An example of these results is shown in Figure 2(a). Refilled holes and targets were placed in rows along either side of the road being imaged.

Further author information:
A.Z.: azare@cise.ufl.edu, M. S.: miranda.silvious@us.army.mil, R. C.: rrclose@gmail.com, P. G.: pgader@cise.ufl.edu

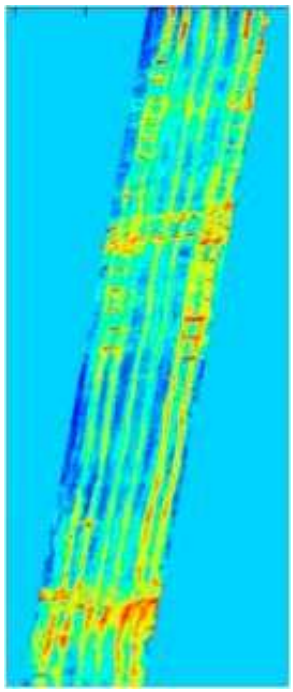

Figure 1. Disturbed earth ratio image computed using the pixel-wise ratio of the first two bands in the MSI data.

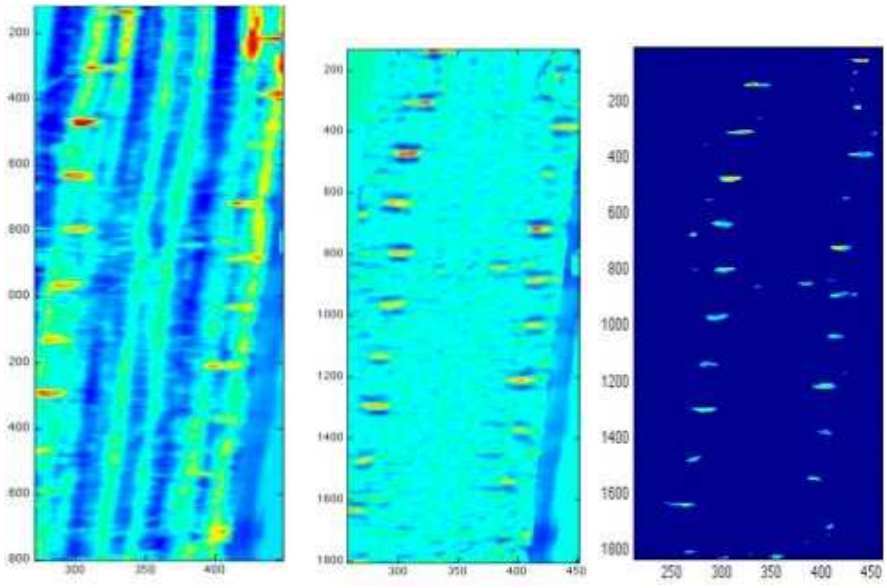

(a) (b) (c)

Figure 2. (a) Anomaly detection results using a double-gated filter on the result of a disturbed earth ration image (b) Background subtraction results obtained following anomaly detection using the double-gated filter. (c) Airborne alarms found by thresholding the background subtraction results shown in (b). Each connected component is marked as an airborne alarm.

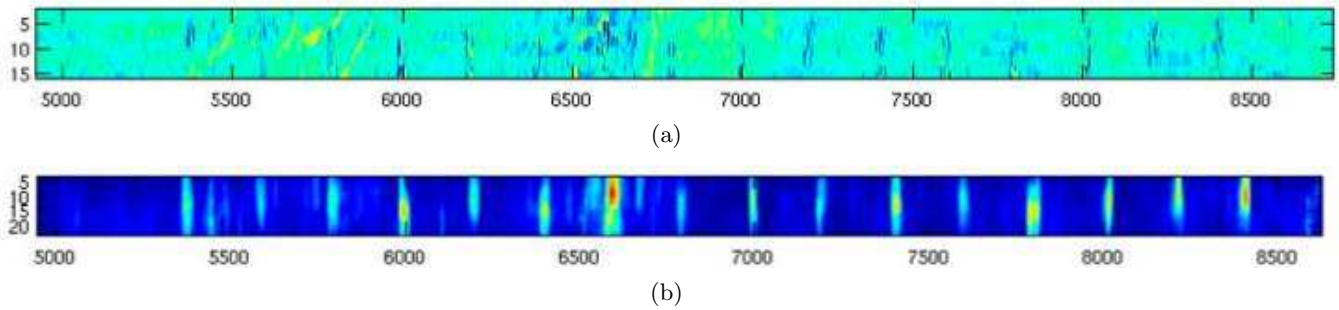

Figure 3. (a) Results following the difference of the maximum and minimum values in the GPR signal for each ground location. (b) Results after computing the local variance at every pixel location over the results shown in (a). Landmines and refilled holes are highlighted in this image.

Following the double gated filter, background subtraction was performed. Background subtraction was performed by subtracting the local mean in a 60x2 pixel window from each pixel in the image. This further removed the disturbed soil features created by vehicle tracks in the road. Examples of the background subtraction results are shown in Figure2(b). The resulting background-subtracted image was thresholded (as shown in Figure 2(c)) and each connected component remaining after thresholding was labeled an alarm in the airborne MSI data.

3. GROUND PENETRATING RADAR ANALYSIS

The GPR data was also processed to create a disturbed soil feature image. The GPR data contains a "ground-bounce" signature associated with the GPR data corresponding to the ground surface. The GPR disturbed soil feature is based on the observation that the ground-bounce signature changes over areas of disturbed soil.[1] Since ground bounce signatures tend to dominate the GPR signal, the GPR disturbed soil feature is computed by subtracting the maximum and minimum values of the GPR signature at every ground location and then computing the variance in a local window for each pixel location. Examples of the GPR disturbed soil feature results are shown in Figures 3(a) and 3(b).

In addition to computing the GPR disturbed soil feature, four detection algorithms for Ground Penetrating Radar were considered: a hidden Markov model (HMM)[2,3] and 3 different pre-screeners, PS1, PS2, PS3.[4–6] After finding airborne alarms using the method described above, GPR alarms were cued if they fell within a 1 meter halo of an airborne alarm. If several GPR alarms fell within a 1 meter halo of an airborne alarm, one alarm was selected and the remaining alarms were ignored. The ignored alarms were not counted as a false alarms or detections in the final results.

4. RESULTS

Results were scored over approximately 0.5 linear kilometers. In the scored area, there were two target types with 18 targets of type 1, 20 targets of type two and 25 refilled holes. The results considering each of the four algorithms are shown. In Figure 4, results are shown in which refilled holes were ignored during detection results. Therefore, detections within one meter of a refilled hole were ignored and not considered a detection nor a false alarm. For each of the ROC (receiver operating curves) in this paper, the x-axis corresponds to false alarms per meter squared and the y-axis corresponds to probability of detection. In each of these plots, four curves are shown. The red curve corresponds to the not cued GPR algorithm results. The blue curves corresponds to the cued GPR results. The black curve corresponds to the airborne alarm results and the green curve corresponds to the fused results (geometric mean of the features values) with the airborne alarms and the cued GPR alarms. Overall, cued GPR results were generally improvements over the not cued GPR results indicating there may be benefit in using airborne MSI data to cue the GPR algorithms for detection of buried targets. In Figure 4(b), the cued GPR results did not have any false alarms and, therefore, cannot be seen on the plot since the ROC curve is a vertical line coincident with the y-axis. Figures 4(d) and 5(d) correspond to the HMM results on this data.

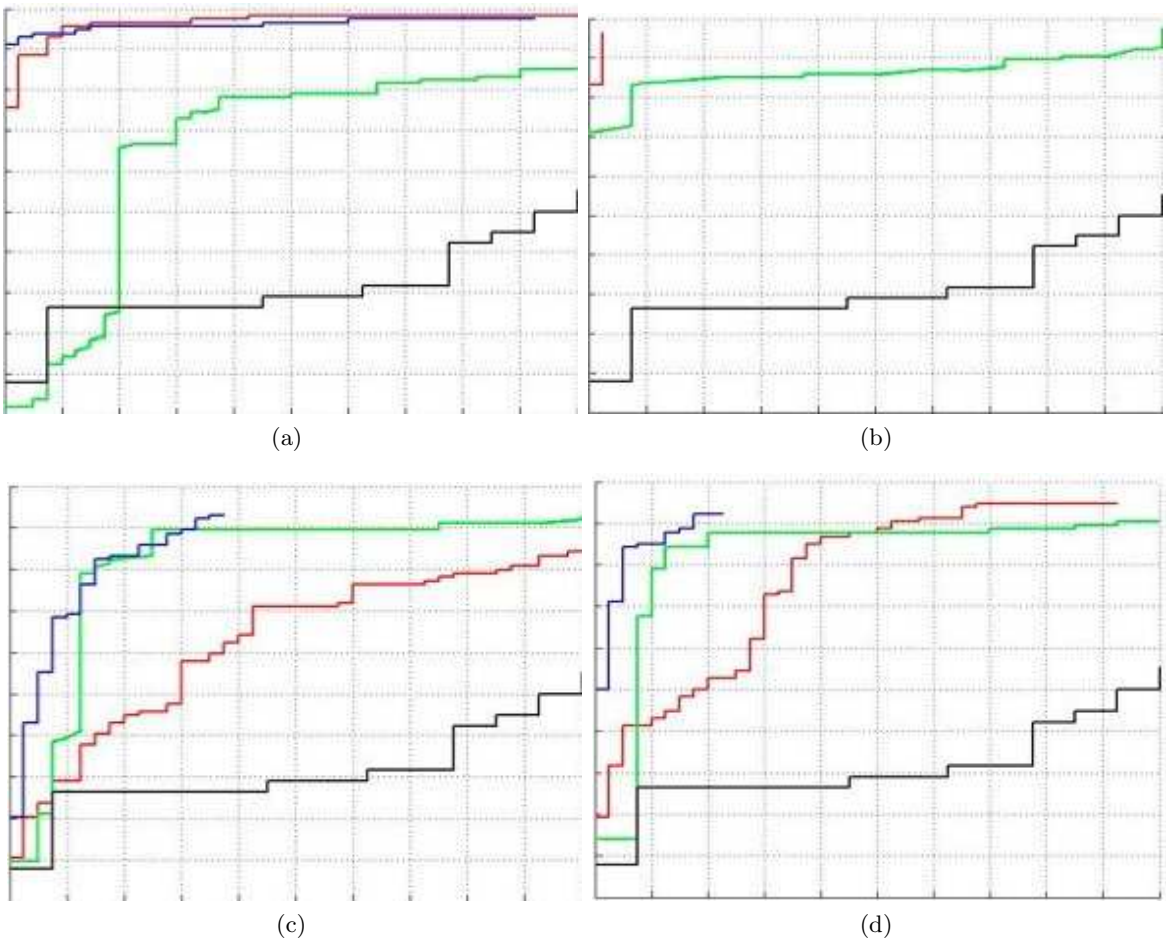

(a) (b)

(c) (d)

Figure 4. ROC Curves for each of the four GPR algorithms in which refilled holes are ignored in detection results. Detection within a one meter halo of a refilled hole is not considered a detection nor a false alarm. In each of these plots, the red curve corresponds to the not cued GPR algorithm results, the blue curves corresponds to the cued GPR results, the black curve corresponds to the airborne alarm results and the green curve corresponds to the fused results (geometric mean of the features values) with the airborne alarms and the cued GPR alarms.

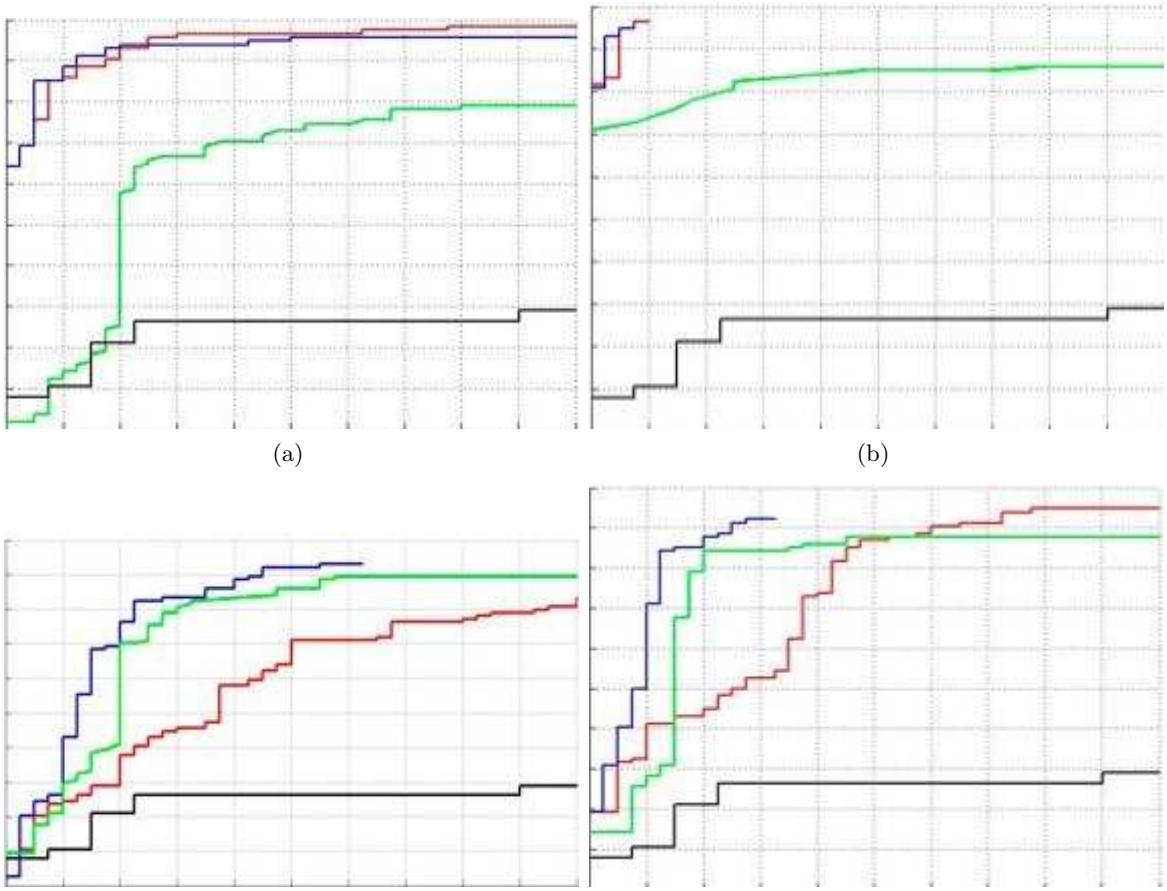

(a) (b)

(c) (d)

Figure 5. ROC Curves for each of the four GPR algorithms in which refilled holes were considered false alarms. Detection within a one meter halo of a refilled hole is considered a false alarm. In each of these plots, the red curve corresponds to the not cued GPR algorithm results, the blue curves corresponds to the cued GPR results, the black curve corresponds to the airborne alarm results and the green curve corresponds to the fused results (geometric mean of the features values) with the airborne alarms and the cued GPR alarms.

ACKNOWLEDGMENTS

The authors are grateful to the many people who contributed to collection of this dataset. The University of Florida research was accomplished under Cooperative Agreement Number DAAD19-02-2-0012. The views and conclusions contained in this document are those of the authors and should not be interpreted as representing the official policies, either expressed or implied, of the U. S. Government. The U. S. Government is authorized to reproduce and distribute reprints for Government purposes notwithstanding any copyright notation hereon.

REFERENCES

[1] Rosen, E. and Ayers, E., "Fusion of disturbed soil feature for down-looking ground-penetrating radar mine detection," in [*Detection and Remediation Technologies for Mines and Minelike Targets XII*], Harmon, R. S., John H. Holloway, J., and Broach, J. T., eds., *Proc. SPIE* **6553** (May 2007).

[2] Frigui, H., Ho, K., and Gader, P. D., "Real-time land mine detection with ground penetrating radar using discriminative and adaptive hidden markov models," *EURASIP Journal on Applied Signal Processing* **2005**, 1867–1885 (July 2005).

[3] Gader, P. D., Mystkowski, M., and Zhao, Y., "Landmine detection with ground penetrating radar using hidden markov models," *IEEE Trans. Geoscience and Remote Sensing* **2001**, 1231–1244 (June 2001).

[4] Torrione, P. A., Collins, L. M., Clodfelter, F., Frasier, S., and Starnes, I., "Application of the lms algorithm to anomaly detection using the wichmann/niitek ground-penetrating radar," in [*Detection and Remediation Technologies for Mines and Minelike Targets VIII*], Harmon, R. S., John H. Holloway, J., and Broach, J. T., eds., *Proc. SPIE* **5089**, Sept.

[5] Frigui, H., Zhang, L., and Gader, P. D., "Context dependent multi-sensor fusion and its application to land mine detection," *IEEE Trans. Geoscience and Remote Sensing* . Accepted.

[6] Frigui, H., Zhang, L., Gader, P. D., Wilson, J. N., Ho, K. C., and Mendez-Vazquez, A., "An evaluation of several fusion algorithms for anti-tank landmine detection and discrimination," *Information Fusion* . Accepted.